Semiclassical description of proton stopping by atomic and molecular targets

W. A. Beck*
Department of Physics, Box 351560, University of Washington, Seattle, Washington 98195-1560 and MicroSound Systems, Issaquah, Washington 98027

L. Wilets†
Department of Physics, Box 351560, University of Washington, Seattle, Washington 98195-1560
(Received 27 August 1996)

In recent years there has been renewed interest in semiclassical methods of modeling atomic structure and collision dynamics. A class of many-body models applied to these problems are descendants of the original work by Kirschbaum and Wilets [Phys. Rev. A **21**, 834 (1980)], who used momentum dependent pseudopotentials to exclude particles from quantum mechanically forbidden regions of phase space. These methods have been used for static, ground-state calculations for increasingly complex atoms, but the calculation of collision cross sections has to date been limited to fairly simple systems. This paper will consider the dependence of collision cross-section calculations on the parameters of the Kirschbaum-Wilets semiclassical model, present a general method for calculation of proton stopping powers by atomic targets, and present results for proton stopping by atomic targets ranging from He to Ne which agree quite well with experiments over a wide range of proton energies. A simple extension of the method to multicenter molecular targets will then be discussed, illustrated by the case of proton stopping by water. [S1050-2947(97)01004-4]

PACS number(s): 34.90.+q, 02.70.Ns, 34.50.Bw

I. INTRODUCTION

Classical trajectory Monte Carlo (CTMC) calculations of charged particle collisions, in which collisions are calculated microscopically and then averaged over an ensemble of initial conditions, have long been used to model collision processes in simple systems. Early work on single electron targets was performed by Abrines and Percival [1,2], and Olson and Salop [3]; later Olson [4] extended his earlier work to look at the state distributions resulting from electron transfer from H to fully stripped ions, and Cohen [5] applied the method to muon capture by H.

Becker and MacKellar [6] and Pfeifer and Olson [7] attempted to extend the approach to two electron systems, with mixed results. The lack of any quantum mechanics in the CTMC approach apparently limited it to systems in which, by definition, quantum effects played a small role, e.g., single heavy charged particle collisions with very simple targets such as H, He^+, etc., or in which one active electron was treated classically in the mean field of the rest of the target.

The lure of applying the many-body Monte Carlo approach to more complex systems, in which many-body effects could not be neglected but which were too complicated for a full quantum-mechanical treatment led to what could be termed a semiclassical trajectory Monte Carlo (STMC) approach, which added a numerical model of quantum effects to the purely classical trajectory calculations of CTMC. In a classical model of multielectron atomic targets, outer electrons evaporate while inner electrons collapse into the nucleus. To stabilize and structure the many-body atomic model, and thus allow its use as a target in collision simulations, Kirschbaum and Wilets [8] proposed excluding the atomic electrons from regions of phase space which are forbidden by the Heisenberg and Pauli principles by using momentum-dependent pseudopotentials of the general form

$$V=\frac{\xi^2}{4\alpha r^2}\exp\{\alpha[1-(rp/\xi)^4]\}. \tag{1}$$

Here, ξ is the size of the forbidden region of phase space and α is the hardness of the exclusion (strictly speaking, the size of the excluded region is $\xi/\alpha^{1/4}$, but the principle role of α is as the strength of the exclusion).

This approach was originally developed to study nuclear structure and collisions [9–12]. Zaijfman and Maor [13] used the model to study atomic He targets. Further work on He-scale problems was carried out by Lerner, LaGattuta, and Cohen [14–16] and recently by Cohen [17], while Dorso and Randrup [18] looked further at nuclear applications; often the later work included variations in the form of the semiclassical core terms. We applied this method to study the capture of antiprotons on He [19].

As with the previous CTMC work, however, early efforts to extend STMC atomic collision calculations to complex systems, i.e., to greater than two electrons, met with limited success. This was due in part to the limited availability of computational resources; quite understandably, much of the earlier work in this field was optimized to reduce CPU time at the expense of a fuller exploration of the collision model. The recent explosion in the availablity of lower cost computer power has allowed a fuller examination of the STMC approach, resulting in a better understanding of its characteristics as a calculational tool. In particular, the ability to perform collision calculations from a greater number of properly distributed Monte Carlo initial conditions has increased

*Electronic address: beck@nucthy.npl.washington.edu
†Electronic address: wilets@nuc2.npl.washington.edu

insight into the nature of the semiclassical pseudopotentials fundamental to the STMC approach, and their effects on collision calculations. The calculation of proton stopping powers illustrates the principal features of the method.

II. THE SEMICLASSICAL MODEL OF AN ATOM

Using atomic units, with $\hbar = e = m_e = 1$, the classical model of an N electron atom of atomic number Z is described by the Hamiltonian

$$H_{cl} = T + V_z + V_{ij} = \sum_{i=1}^{N} \left[\frac{p_i^2}{2} - \frac{Z}{r_i} \right] + \sum_{i<j} \frac{1}{r_{ij}}, \tag{2}$$

where $\vec{r}_i$ and $\vec{p}_i$ are the positions and momenta of the atomic electrons relative to the fixed nucleus and $r_{ij} = |\vec{r}_i - \vec{r}_j|$ are the relative coordinates of electron pairs.

The semiclassical, Kirschbaum-Wilets version of this model is described by

$$H_{sc} = H_{cl} + V_H + V_P = H_{cl} + \sum_{i=1}^{N} V_H(r_i, p_i) + \sum_{i<j} V_P(r_{ij}, p_{ij}), \tag{3}$$

where

$$V_H(r_i, p_i) = \frac{\xi_H}{4\alpha_H r_i^2} \exp\{\alpha_H [1 - (r_i p_i / \xi_H)^4]\} \tag{4}$$

is a Heisenberg-type pseudopotential which stabilizes the atom by preventing collapse of the atomic electrons into the nucleus, while

$$V_P(r_{ij}, p_{ij}) = \frac{\xi_P}{4\alpha_P r_{ij}^2} \exp\{\alpha_P [1 - (r_{ij} p_{ij} / \xi_P)^4]\} \delta_{s_i s_j} \tag{5}$$

is a Pauli-type pseudopotential which separates identical electron pairs in phase space, resulting in an electronic structure.

The semiclassical model of an atom can be minimized to find a stable ground state in which the electrons, while at rest, have nonzero momenta in the presence of momentum dependent pseudopotentials; this process has been recently reviewed by Cohen [20], who calculated ground states up to $Z = 38$ with fixed parameters defining the pseudopotentials. In using the model to study collision systems we look further into the dependence of both the ground-state electron distributions and of the resulting collision dynamics on the pseudopotential parameters α and ξ.

A. Semiclassical model of He: Nature of the Heisenberg core

Consider He: with two electrons in antiparallel spin states our semiclassical Hamiltonian adds only V_H to the classical description, and the minimum energy configuration consists of two stationary electrons on opposite sides of the nucleus, each with a nonzero momentum of magnitude $p_i = \xi_H \neq dr_i/dt$. Figure 1 illustrates the nature of semiclassical He ground states as a function of the Heisenberg core:

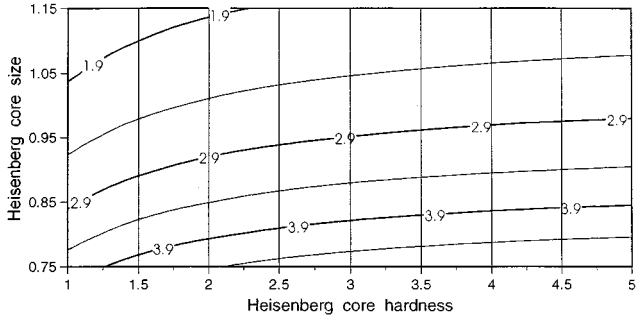

FIG. 1. Semiclassical He binding energy as a function of Heisenberg core size (ξ_H) and hardness (α_H).

(i) As the size of the core increases, the equilibrium phase-space separation of the electrons from the nucleus increases and the total ground-state binding energy decreases.

(ii) For a given core size, as the core becomes harder the value of the total binding energy increases asymptotically to a value determined by the core size.

Fixing the total binding energy of the model at the experimental value of 2.9 a.u. $\sim$78.9 eV, i.e., confining the Hamiltonian to the $E = 2.9$ binding energy contour of Fig. 1, leaves a single free parameter in the Hamiltonian. Figure 2 details the components of the ground-state energy as a function of α_H along this contour:

(i) The nature of the ground state changes only gradually along the fixed energy contour; all systems have a constant electron radius $r_{sc} \sim 0.603$, which compares well with the electron mean radius, $\langle r \rangle_{He} \sim 0.59$, and as a result total Coulomb potential energy is constant at $V_{Coulomb} = V_z + V_{ij} \sim -5.8$.

(ii) Somewhat paradoxically, as the value of the Heisenberg core size and hardness increase, the value of the Heisenberg energy in the ground-state Hamiltonian decreases as the Heisenberg pseudopotential more strongly excludes the electrons from the phase-space region of the nucleus and the ground-state momentum of the electrons increases.

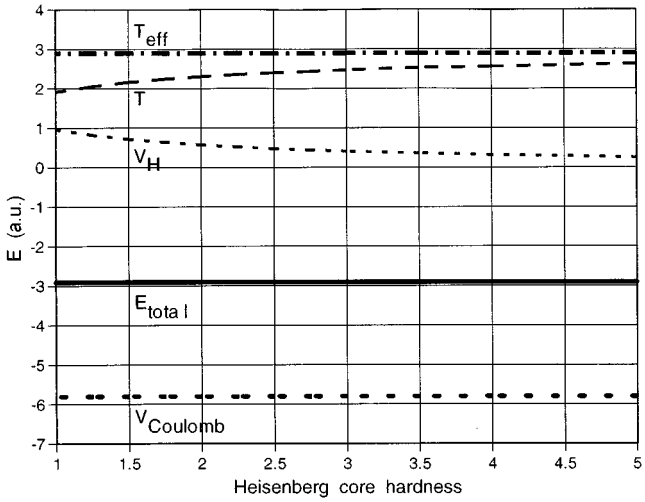

FIG. 2. Semiclassical He ground-state energy components as a function of core hardness α_H for systems with the correct total ground-state binding energy.

(iii) The model obeys a virial theorem. With the effective kinetic energy of this system defined as $T_{eff}=T+V_H$, the total ground-state energy is minimized at

$$E_{total}=V_{Coulomb}+T_{eff}=(V_z+V_{ij})+(T+V_H)=V_{Coulomb}/2 =-T_{eff}. \quad (6)$$

This is true, in general, for our semiclassical Hamiltonian including both Heisenberg and Pauli cores. Since p scales as $1/r$ and the pseudopotentials are of dimension $1/r^2=p^2$, we write

$$H_{sc}(\{r_i\},\{p_i\})=V_{Coulomb}(\{r_i\})+T_{eff}(\{r_i\},\{p_i\}), \quad (7)$$

with

$$T_{eff}=T+V_H+V_P =\sum_i \frac{p_i^2}{2}+\sum_i \frac{1}{r_i^2}f_H(r_i p_i)+\sum_{i<j}\frac{1}{r_{ij}^2}f_P(r_{ij}p_{ij}). \quad (8)$$

Then for arbitrary scaling $r\rightarrow\lambda r,\ p\rightarrow p/\lambda$,

$$H_{sc}\rightarrow \frac{V_{Coulomb}}{\lambda}+\frac{T_{eff}}{\lambda^2}, \quad (9)$$

with

$$\frac{\partial H}{\partial\lambda}=\left(\frac{-2\,T_{eff}}{\lambda^3}-\frac{V_{Coulomb}}{\lambda^2}\right)\Bigg|_{\lambda=1}=0\Rightarrow -2\,T_{eff}=V_{Coulomb}. \quad (10)$$

B. Semiclassical Be: Addition of a Pauli core

The model of a Be atom illustrates the effect of the Pauli pseudopotential V_P on the semiclassical ground state. With only the Heisenberg pseudopotential, the Be model minimizes to a ground-state configuration which, with the electrons in a tetrahedron at equal radii around the nucleus, behaves much like the semiclassical He atom.

The addition of a Pauli core to the model splits the ground-state electrons into inner and outer pairs, as shown in Fig. 3(a). Note that the splitting of the electron pairs occurs more quickly for a softer Pauli core; as with the case of the central Heisenberg core, see Fig. 2, the softer interelectron core results in a greater interaction between the electrons and thus a greater separation. Note also that as the size of the Pauli core ξ_P increases, the binding energy of the inner electrons quickly reaches an equilibrium level as they are squeezed in against the central Heisenberg core, while that of the outer electrons continues to decrease as they are pushed further away from the nucleus; clearly, too large a Pauli core will result in valence electrons that are too loosely bound to serve in a realistic model of an atom.

Figure 3(b) reveals how the addition of the Pauli core decreases the total binding in the system, spreading out the electrons in phase space as it splits the electron pairs. In order to achieve the correct total binding energy, the size and strength of the Heisenberg and Pauli pseudopotentials must be adjusted in concert; calculation of collision cross sections provides guidance into how to do this.

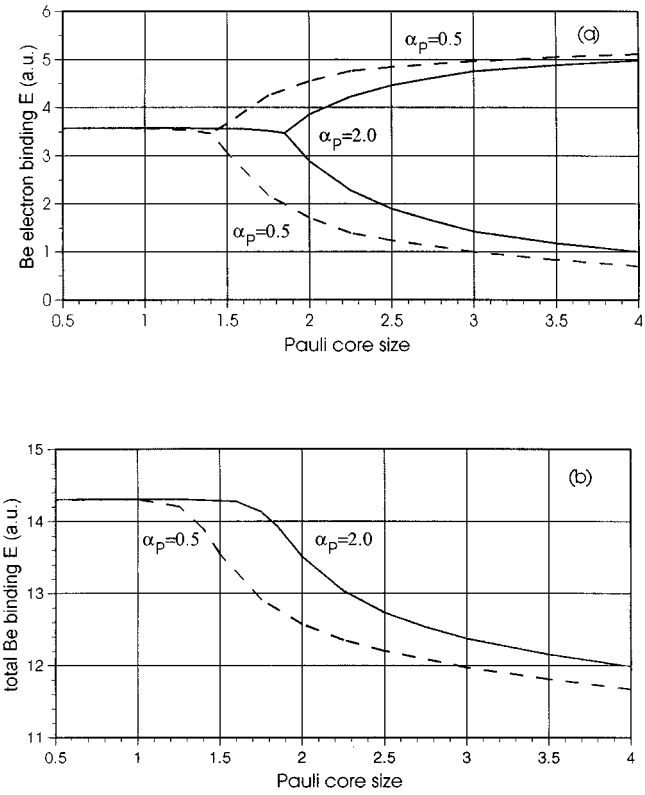

FIG. 3. Splitting (a) of the inner and outer electron energy levels as the Pauli core size ξ_P is increased in the semiclassical Be atom; reduction of the total Be binding energy (b) as the Pauli core spreads the electrons out in phase space.

III. SEMICLASSICAL COLLISION CALCULATIONS: STOPPING POWER

Stopping power, or energy-loss cross section, was originally described by the Bethe theory [21],

$$S=\frac{4\pi Z_1^2 Z_2^2}{m_e v_1^2}\left[\ln\left(\frac{2E_{0,1}}{I}\right)-\ln(1-\beta^2)-\beta^2-\frac{C}{Z_2}\right], \quad (11)$$

where Z_1, Z_2 are the charge of the projectile and target, v_1 is the projectile velocity, $E_{0,1}$ is the initial projectile energy and $\beta=v/c$. I, the mean ionization energy of the target atom, characterizes how free the target atom's electrons are to exchange momentum with the projectile, and is the central parameter in the theory; C/Z_2 are semiempirical shell corrections to the target atom's electronic structure.

This formula works well at higher collision energies, however at lower energies, where stopping powers peak as the projectile velocities approach that of the target electrons and the target-projectile interactions become more complex, and often result in ionization, approximating the electron structure with a single mean ionization term proves inadequate, even with shell corrections.

Various methods of approximating the quantum mechanics of this interaction have been developed for different velocity regimes; the general technique is to consider the target atom in some mean field within which limited collision dynamics can be calculated. Ziegler, Biersack, and Littmark [22] provide a nice history of early work in this area. In an

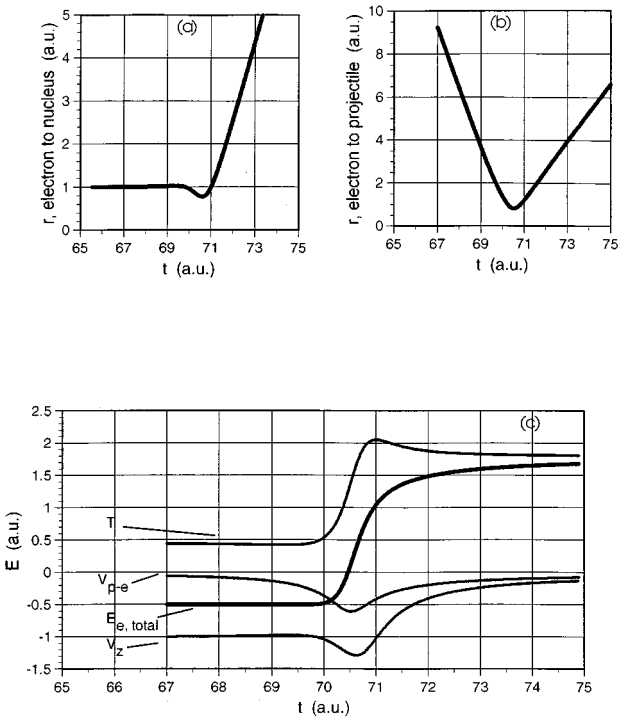

FIG. 4. Time evolution of electron-nuclear radius (a), electron-proton radius (b) and electron binding energy (c) during a high-energy-loss collision between a proton and a soft semiclassical H atom.

alternate approach, Feldmeier [23] coined the term Fermi molecular dynamics to describe his method of following the time evolution of colliding Gaussian wave packets. A recent review of the field is found in Grande and Schiwietz [24], who modeled the complicated interactions in the region of maximum stopping using large numbers of single electron wave functions. For more than fairly simple targets, e.g., H, H_2, He, the analytical approaches founder in the region of maximum stopping, and stopping powers are generally estimated by an empirical curve fit to experimental data; Ziegler, Biersack, and Littmark have carried this approach out to a high degree of sophistication for positively charged projectiles, producing annual refinements to their TRIM (Transport of Ions in Matter) software [25]. Our reference experimental curves for atomic stopping are taken from here and from Andersen and Ziegler's earlier compilation of the experimental data [26].

In contrast to the traditional mean-field and empirical methods, the STMC approach microscopically follows a series of projectile collisions with a fully detailed model of the target atom. Uniquely, this method directly includes electron correlation effects for much larger target systems than can be handled with even the most simplified quantum-mechanical approaches, extending the useful range of the model to lower collision energies and larger target systems.

A. Semiclassical stopping power

The total Hamiltonian for a proton colliding with a fixed nucleus semiclassical atom is given by

$$H_{sc+p}=H_{sc}+\frac{P^2}{2M}-\frac{Z}{R}-\sum_{i=1}^{N}\frac{1}{|\vec{r}_i-\vec{R}|}, \tag{12}$$

where $\vec{R},\vec{P}$ are the coordinates of the proton relative to the nucleus. To model collisions, the classical equations of motion for this system

$$\frac{dx_i}{dt}=\frac{\partial H}{\partial p_i}, \quad \frac{dp_i}{dt}=-\frac{\partial H}{\partial x_i} \tag{13}$$

are solved for $\vec{r}_i,\vec{p}_i$ and $\vec{R},\vec{P}$ over time. Note that there is no pseudpotential term $V_{H,p}(|\vec{r}_{i,p}|,|\vec{p}_{i,p}|)$ between the proton and the target electrons; V_H is used only to stabilize the target system, and all interactions between the target and the projectile are via the Coulomb forces.

Quantum uncertainty is rolled into the model by averaging over a sequence of collision calculations using Monte Carlo initial conditions:

(i) A microcanonical distribution of target configurations is generated by random rotation and parity inversion of the ground-state electron positions and momenta [1].

(ii) Each collision with one of these target configurations is started from an impact parameter b randomized with equal areas πdb^2 up to some maximum value b_{max}.

(iii) The same Monte Carlo seed is used for sequences of collisions from a series of initial proton energies, allowing calculation of collision cross sections as a function of initial projectile energy from repeatable ensembles of initial conditions.

By averaging over an appropriate set of initial conditions one hopes to extract physically meaningful results from microscopically following this semiclassical model of a quantum-mechanical system. For N collisions starting with initial energy E_0 and impact parameters randomized with equal areas up to some b_{max}, the total energy-loss cross section or stopping power, $\sigma\Delta E$, is calculated from the average proton energy loss as

$$\sigma\Delta E(E_0)=\pi b_{max}^2\frac{1}{N}\sum_{i=1}^{N}\Delta E_i(E_0), \tag{14}$$

with an uncertainty

$$\delta(\sigma\Delta E)=\pi b_{max}^2\left[\frac{1}{N}(\langle(\Delta E_i)^2\rangle-\langle\Delta E_i\rangle^2)\right]^{1/2}. \tag{15}$$

B. Close encounter collision dynamics: Influence of core hardness

In a typical series of $N\sim$ a few thousand or so collisions much of the actual stopping occurs in a small fraction of the collisions in which the proton and one of the target electrons collide nearly head-on, with a large component of collinear momenta, i.e., aligned for high-momentum exchange. The nature and frequency of these approximately head-on collisions are central to correct calculation of overall stopping powers; their details reveal the importance of core hardness in collision dynamics, and thus its significance to the use of STMC techniques for collision modeling.

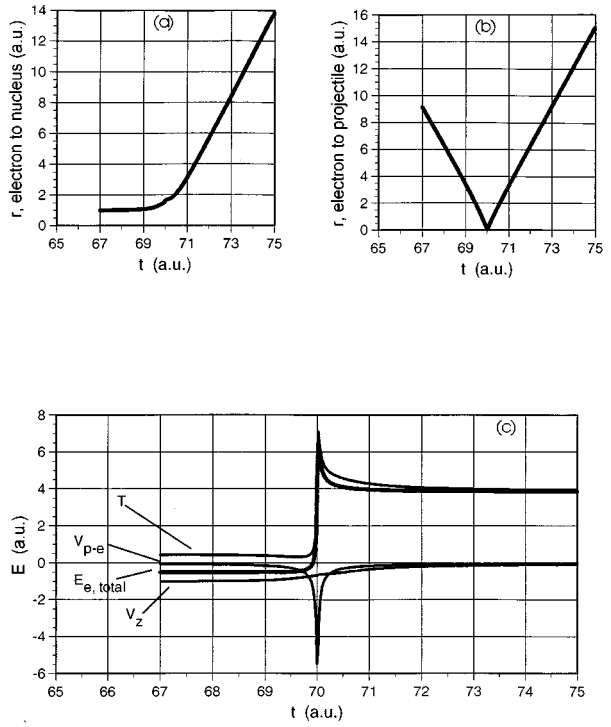

FIG. 5. Time evolution of electron-nuclear radius (a), electron-proton radius (b), and electron-binding energy (c) during a high-energy loss collision between a proton and a hard semiclassical H atom.

Consider, for simplicity, an example of a typical high-energy-loss collision between a proton and our semiclassical H atom. Figures 4 and 5 plot the time evolution of this collision for H targets incorporating both soft ($\alpha_H=1$) and hard ($\alpha_H=5$) Heisenberg cores: Figs. 4(a) and 5(a) plot the radius of the electron relative to the nucleus of the H atom, Figs. 4(b) and 5(b) the distance betwen the target electron and the colliding proton, and Figs. 4(c) and 5(c) the components of the electron energy in the collision system.

Figure 6 plots the ground-state energy as a function of electron radius for both the soft and hard H atoms; the different collision dynamics of Figs. 4 and 5 are a result of the different shapes of the energy wells confining the electron. In

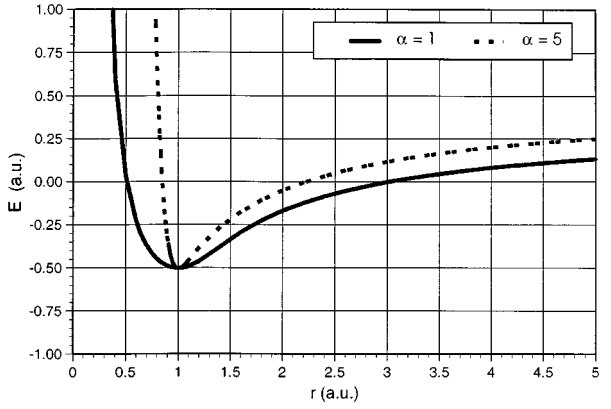

FIG. 6. Ground-state energy as a function of electron radius for semiclassical H atoms incorporating soft ($\alpha_H=1$) and hard ($\alpha_H=5$) Heisenberg cores.

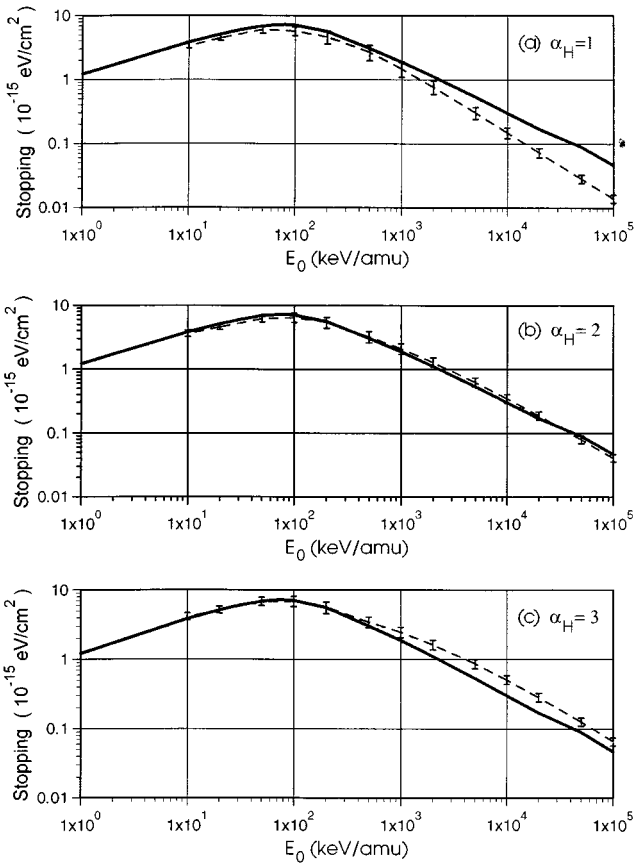

FIG. 7. Semiclassical He stopping powers for Heisenberg core size = 1.0 (a), 2.0 (b), and 3.0 (c).

Fig. 4 the softer target H atom is deformed during the collision as the electron in the softer potential well begins to acquire momentum from the colliding proton and is swung around into the nucleus. This process peaks at the closest encounter of the proton and the target electron, which is simultaneously the point at which the electron is deflected furthest into the soft Heisenberg core of the semiclassical nucleus. Note that the energy changes in the soft collision system are smooth and continuous as the proton loses about 2.2 a.u. of kinetic energy in ionizing the electron from its ground-state energy of -0.5 to its continuum energy of ~ 1.7; in particular, note that because of the target deformation $V_{p-e}=-1/|\vec{r}-\vec{R}|$, the Coulomb attraction between the projectile and the target electron, remains well behaved.

In contrast, as the proton collides with the $\alpha_H=5$ target atom in Figs. 5, the narrower, steeper-sided potential well which results from the harder Heisenberg core holds the electron more rigidly in place and prevents the atom from absorbing the shock of the collision by deforming as above. The colliding proton gets much closer to the target electron and thus transfers more momentum to it before finally whipping it out at a much higher velocity than in the softer collision. Note that the energy transfer in this collision system is much more abrupt as the proton loses about 4.5 a.u. of kinetic energy in ionizing the the electron to its final continuum state of $E\sim 4$; note, in particular, the singular nature of V_{p-e} and the kinetic energy T (and thus of the total electron energy) during the closer encounter of the projectile and

the electron localized in the bottom of the harder potential well.

The additional energy loss resulting from the hard-core collision dynamics, though occuring infrequently, turns out to be a source of significant error in net stopping power calculations. Though the ground-state energy curves and the collision dynamics in more complex target systems are complicated by additional electron interactions, in all the systems which we have studied, close encounter collisions similar to the above remain the predominant factor in net stopping powers, which thus depend directly on correct selection of pseudopotential hardness.

C. Frequency of close encounter collisions: Monte Carlo considerations

The frequency of the important, approximately head-on collisions is governed by the Monte Carlo selection of initial target configurations and impact parameters. In our early work on this problem using harder semiclassical pseudopotentials ($\alpha \sim 5$, typically), undersampling of the collision configuration space resulted in initially promising results for which, rather annoyingly, both the statistical uncertainty and the deviation from experimental results often grew as the sample size increased and/or the sample seed was changed. In particular, limiting the maximum impact parameter or segmenting the range of impact parameters, both of which have in the past been standard techniques to conserve CPU time, often significantly increased the errors in our calculations, hiding the α dependence of the stopping power. We found that continuously sampling the full impact-parameter space up to b_{max}, chosen so that the final result was not b_{max} dependent, led most directly to collision cross sections which converged as we more densely sampled the collision configuration space with multiple seeds.

D. Energy accounting

In addition, correct calculation of stopping powers requires correct calculation of initial and final proton energies relative to the target system; particularly at higher projectile energies, where stopping is smaller, small systematic errors will accumulate into significant errors in the final result.

Since stopping powers are measured as a function of the initial energy of the colliding proton, we have specified that energy at the proton radius $R=\infty$, then adjusted the actual starting energy of the collision for the starting point of the collision at $R=R_0$. Since the total energy of the collision system is that of the target plus that of the proton, wherever the proton is relative to the target system,

$$E_{p,R=R_0}+E_{tgt,R=R_0}=E_{p,R=\infty}+E_{tgt,R=\infty}, \tag{16}$$

the initial energy of the proton at the start of the collision is simply

$$E_{p,R=R_0}=(E_{p,R=\infty}+E_{tgt,R=\infty})-E_{tgt,R=R_0}. \tag{17}$$

For simple collisions in which the proton collides with the target atom without picking up an electron, the final proton energy is calculated in a similar fashion. Particularly at lower energies, however, the important, high-energy-loss collisions often include electron transfer, and calculating the overall stopping power requires correctly calculating the final proton kinetic energy in the newly formed H atom, which will have interesting dynamics of its own. Initially we evaluated this by taking the time average of the proton energy, but found it computationally inefficient to sample densely enough to avoid aliasing the often high-frequency orbits of the newly formed H atom. A more accurate and efficient method is to calculate the final proton energy from the center-of-mass velocity of the newly formed H atom, which in this semiclassical system is not simply P_{cm}/M_{cm}, but rather

$$\vec{V}_{cm}=\frac{M_p\vec{V}_p+\vec{v}_e}{M_{cm}}, \tag{18}$$

with

$$\vec{V}_p=\vec{\nabla}_P H, \quad \vec{v}_e=\vec{\nabla}_p H. \tag{19}$$

IV. STOPPING POWER RESULTS, He THROUGH Ne

The relatively simple case of proton stopping by He illustrates the effect of pseudopotential core strength on stopping power. Figures 7(a)–7(c) compare experimental He proton stopping powers to our semiclassical calculations for different Heisenberg core strengths, $\alpha_H=1.0-3.0$, i.e., for systems described along the α_H axis of Fig. 2. Each point on each of these curves is calculated from a total of $N=3000$ collision simulations, using a repeating ensemble of initial conditions chosen as described above. These curves show that at higher energies, where the simple proton electron collision dominates the energy-loss process, collision calculations performed using semiclassical targets stabilized by a softer Heisenberg core underestimate stopping power, while those using a harder Heisenberg core overestimate it, with the correct balance achieved at $\alpha_H \sim 2$. At lower collision energies, as proton and electron velocities, i.e., p/m, become comparable this sensitivity to core hardness is reduced.

As discussed above, a Pauli core provides structure to the semiclassical model of more complex atoms by holding identical electrons apart in phase space. Figure 8(a) shows the proton stopping power of a semiclassical Be atom incorporating only a Heisenberg pseudopotential, with the electrons in a tetrahedron at equal distances from the nucleus. Here, the choice of $\alpha_H=2.0$ again results in correct stopping powers at the higher impact energies, but at lower energies what should be the outer electrons are too tightly bound and do not interact realistically with the projectile.

As shown in Fig. 8(b), addition of a Pauli pseudopotential of core size $\xi_P=2.0$ and core hardness $\alpha_P=1.0$ results in correct stopping powers up to $E_0 \sim 100$ keV, the region of peak energy loss. These values for the Pauli core were determined by cross-section fitting and analysis of collision dynamics similar to that described above for the Heisenberg core, and produce a Pauli core which is sufficient to separate the electrons into a reasonable shell structure but not so large or strong as to unduly distort the collision dynamics.

Note that this Pauli core was not chosen to match any particular details of the target atom structure, e.g., correct first ionization potential or average radius of an electron shell; while it is straightforward to adjust the semiclassical

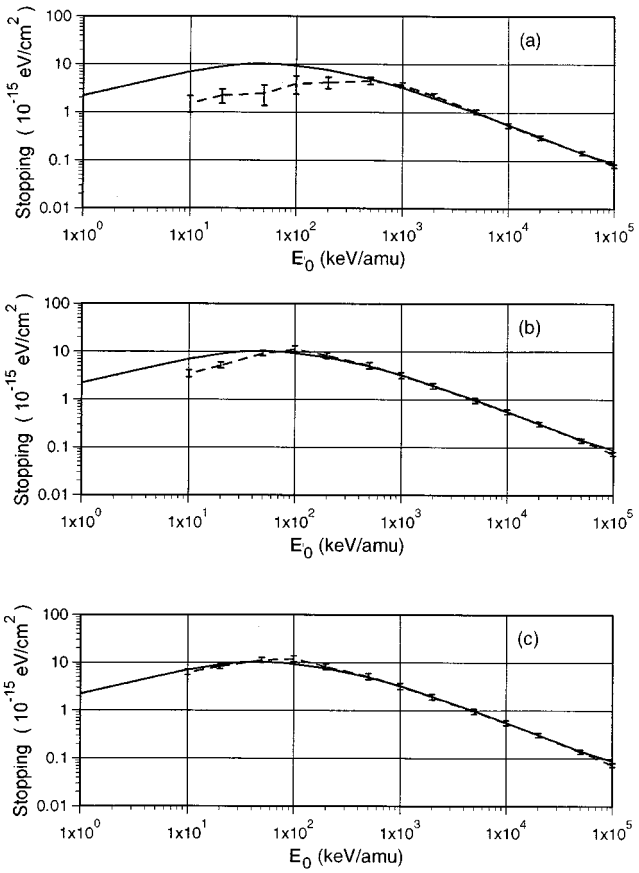

FIG. 8. Stopping powers for semiclassical Be models: (a) including only the Heisenberg pseudopotential; (b) with addition of the Pauli pseudopotential; (c) with center-of-mass calculation of final energies for electron transfer.

model to match any particular detail of the atomic structure, we found this approach particularly unsuccessful in developing a model to be used for collision dynamics. Since the intent of the model was to study charged particle collisions, the Pauli core was chosen to provide an overall structure to the target which, when averaged over an ensemble of collison conditions, would yield accurate stopping powers. Note also that in order to maintain the correct total binding energy, the size of the Heisenberg core was decreased from ~ 1.02 in Fig. 8(a) to ~ 1.01 in Fig. 8(b), to compensate for the slight overall spreading out of the electrons caused by the addition of the Pauli core.

At the lowest collision velocities, a significant fraction of the high-energy-loss collisions result in electron transfer from the target atom to the proton; as discussed above, correct calculation of stopping power requires an accurate value for the final proton energy in the newly formed H atom. Calculating the final proton energy using the center-of-mass method of Eq. (18) provides the final correction to the calculation of lower-energy stopping powers, as shown in Fig. 8(c).

The Heisenberg and Pauli core values determined for He and Be provide a good starting point for modeling proton stopping by larger atomic targets. Our general method of developing a target model is to set the Pauli core to $\alpha_P = 1.0$, $\xi_p = 2.0$, the Heisenberg core hardness to $\alpha_H = 2.0$, and then to adjust the size of the Heisenberg core

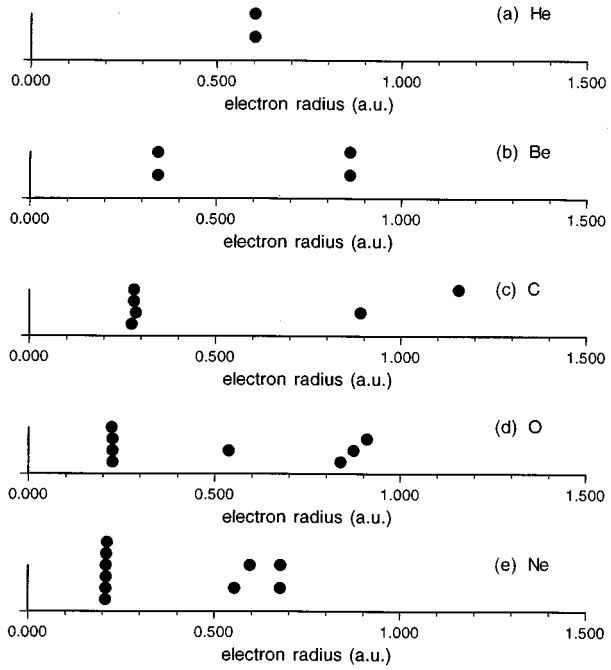

FIG. 9. Radial distribution of semiclassical ground-state electrons for (a) He, (b) Be, (c) C, (d) O, and (e) Ne.

to achieve the correct total binding energy of the system. The best fit stopping powers are obtained by gradually reducing the size of the Pauli core with increasing atomic number, e.g., the base value of $\xi_P = 2.0$ for Be reduces to 1.5 for our C and O models, and to 1.25 for Ne; as with the case of Be, correct total binding energy is restored by a small adjustment to the size of the Heisenberg core.

Note that these semiclassical cores are substantially softer than were used in earlier atomic STMC calculations, which used a core hardness of $\alpha \sim 5$, as was originally developed to model nuclear interactions [8,9]. These softer cores are more appropriate for modeling on the atomic scale, since they result in a well distributed, well behaved set of target electrons with collision dynamics which do not distort stopping cross sections.

Figure 9 presents the radial distribution of electrons for our semiclassical models from He to Ne; Figs. 10(a)–10(c) show the proton stopping powers calculated for the C, O, and Ne targets; the fit to the experimental data remains good for these larger systems. Here a total of 5000 collisions per initial energy were averaged to reduce statistical errors.

The case of Ne is particularly instructive of the effects of too large a Pauli core. Increasing core size to 2.0 results in a single valence electron at a radius of greater than 3 a.u., clearly at odds with the closed shell of the Ne atom; collision interactions with this loosely bound electron significantly distort stopping power calculations. Thus while it it would be pleasing to have a model with a single set of parameters, use of the model for collision modeling precludes this. Upon reflection, it is not surprising that, akin to the shell corrections in the Bethe theory, the semiclassical model also requires a bit of shell correcting.

V. STOPPING BY SIMPLE MOLECULAR TARGETS: H_2O

Calculation of stopping powers by multicentered, molecular targets provides numerous opportunities to complicate the

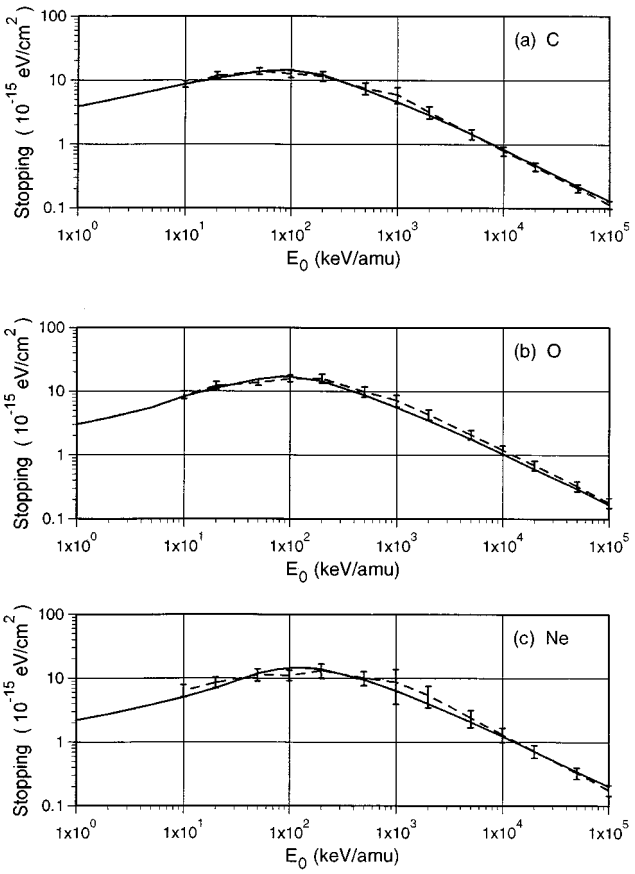

FIG. 10. Semiclassical vs experimental proton stopping powers for (a) C, (b) O, and (c) Ne.

semiclassical model. A first cut approach is to fix the atomic centers, and then to minimize the energy of the electron distribution. While a significant simplification, to the extent that the stopping power is primarily due to projectile-electron interactions it holds some hope of success.

Figure 11 shows an azimuthal projection of the ground-state electron distribution around a fixed center model of an H_2O atom, with the H nuclei fixed at $r \sim 1.01$ Å ~ 1.9 a.u. at an angle of $\sim 104.5°$ from an O nucleus at the origin. Here, the Pauli core determined for O is used, and, as for the atomic case, the electron distribution is adjusted to achieve the correct total binding energy (of $E_{H_2O} \sim 76.5 = E_O + 2E_H + \sim 0.35$ molecular binding) by minor adjustments to the size of the Heisenberg cores.

The proton stopping power for this model is shown in Fig. 12; here the reference curve is calculated from experimental data for H and O as per Ziegler, Bierscak, and Littmark [22]. The fairly good results from our first cut molecular model reflect the predominance of proton-electron interactions in the stopping power. By selecting a reasonable electron distribution and then randomizing it over an ensemble of initial conditions, average stopping power can be calculated fairly accurately.

VI. SUMMARY AND FUTURE PROSPECTS

Semiclassical trajectory Monte Carlo calculations have long represented an enticing possibility to examine collision

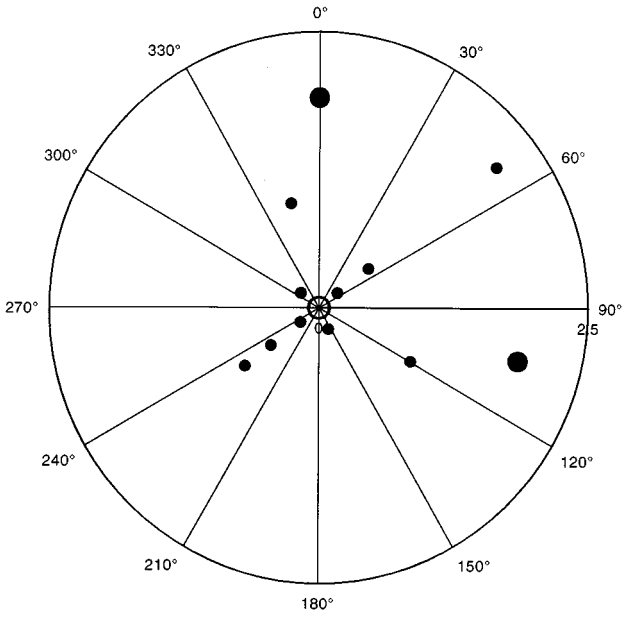

FIG. 11. $r-\phi$ plot of semiclassical fixed center model of H_2O; large dots are H nuclei, smaller dots are electrons.

systems too complex for full quantum-mechanical treatment. By focusing on the dynamic behavior of the model, we have softened the semiclassical pseudopotentials used in the Kirschbaum-Wilets approach, thus eliminating some of the highly nonphysical collision dynamics which have plagued this method in the past. This has significantly increased the range of target sizes and initial projectile energies for which collision calculations can be performed; accurate STMC calculations of proton stopping powers demonstrate the basic suitability of the approach for collision calculations.

Obvious future applications of these techniques are collision systems which are not so well understood as that of protons on atomic targets, in particular, exotic projectiles such as π, μ, and $\bar{p}$ on both atomic and molecular targets, where the details of the slowing and capture of the projectile into exotic atoms are of current interest. The capture of a negative projectile by the target presents additional complications in the final-state analysis, some of which we have discussed previously [19].

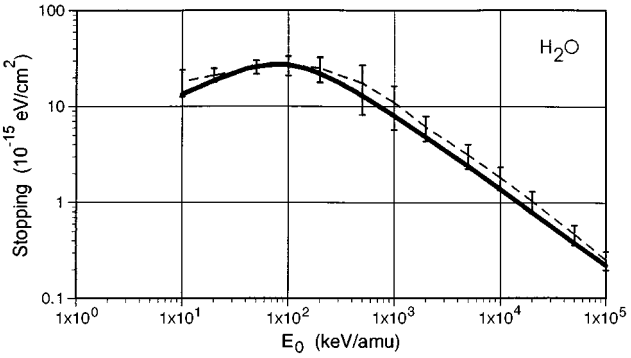

FIG. 12. Semiclassical vs reference stopping powers for protons on H_2O.

Clearly, semiclassical molecular models will have to be more realistic than our first cut fixed center method if they are to be useful for analyzing the capture and cascade dynamics of exotic particles on molecular targets, but the results achieved with the simple approach make us hopeful about the future of this method.

ACKNOWLEDGMENTS

The authors would like to thank George Condo for emphasizing proton stopping power as an appropriate test of the STMC approach; this work stems in large part from that suggestion. We also thank Hans Bichsel and James Cohen for useful discussions.

[1] R. Abrines and I. C. Percival, Proc. Phys. Soc. London **88**, 861 (1966).
[2] R. Abrines and I. C. Percival, Proc. Phys. Soc. London **88**, 873 (1966).
[3] R. Olson and A. Salop, Phys. Rev. A **16**, 531 (1977).
[4] R. Olson, Phys. Rev. A **24**, 1726 (1981).
[5] J. S. Cohen, Phys. Rev. A **26**, 531 (1982).
[6] R. L. Becker and A. D. MacKellar, J. Phys. B **12**, L345 (1979).
[7] S. J. Pfeifer and R. E. Olson, Phys. Lett. A **92**, 175 (1982).
[8] C. L. Kirschbaum and L. Wilets, Phys. Rev. A **21**, 834 (1980).
[9] L. Wilets, E. M. Henley, M. Kraft, and A. D. Mackellar, Nucl. Phys. A **282**, 341 (1977).
[10] L. Wilets, Y. Yariv, and R. Chestnut, Nucl. Phys. A **301**, 359 (1978).
[11] D. Callaway and L. Wilets, Nucl. Phys. A **327**, 250 (1979).
[12] L. Wilets, E. M. Henley, M. Kraft, and A. D. Mackellar, Phys. Rev. Lett. **56**, 320 (1986).
[13] D. Zajfman and D. Maor, Nucl. Phys. A **282**, 834 (1980).
[14] P. B. Lerner, K. LaGattuta, and J. S. Cohen, Laser Phys. **3**, 331 (1993).
[15] P. B. Lerner, K. LaGattuta, and J. S. Cohen, Phys. Rev. A **49**, R12 (1994).
[16] P. B. Lerner, K. LaGattuta, and J. S. Cohen, Phys. Rev. A **50**, 3245 (1994).
[17] J. S. Cohen, Phys. Rev. A **54**, 573 (1996).
[18] C. Dorso and J. Randrup, Phys. Lett. B **232**, 29 (1989).
[19] W. A. Beck, L. Wilets, and M. A. Alberg, Phys. Rev. A **48**, 2779 (1993).
[20] J. S. Cohen, Phys. Rev. A **51**, 266 (1995).
[21] H. Bethe, Ann. Phys. (Leipzig) **5**, 325 (1930).
[22] J. F. Ziegler, J. P. Biersack, and U. Littmark, *The Stopping and Ranges of Ions in Solids* (Pergamon, New York, 1985).
[23] H. Feldmeier, Nucl. Phys. A **515**, 147 (1990).
[24] P. L. Grande and G. Schiwietz, J. Phys. B **28**, 425 (1995).
[25] J. F. Ziegler, TRIM, The TRansport of Ions in Matter, 1995, available from Ziegler@Watson.IBM.com.
[26] H. H. Andersen and J. F. Ziegler, *Hydrogen Stopping Powers and Ranges in All Elements* (Pergamon, New York, 1977).